Dempster-Shafer fusion based building change detection from satellite stereo imagery

Jiaojiao Tian
Remote Sensing Technology Institute
German Aerospace Center (DLR)
Wessling, Germany
Jiaojiao.tian@dlr.de

Peter Reinartz
Remote Sensing Technology Institute
German Aerospace Center (DLR)
Wessling, Germany
Peter.Reinartz @dlr.de

***Abstract*—Building change detection is one of the most essential processing steps for urban monitoring using remote sensing data. As 2D automatic change detection from satellite images is a very challenging task, 3D information, derived e.g. from Digital Surface Models (DSMs) can provide valuable additional information to detect and analyze such changes. In the first step of the proposed approach, a radiometric co-registration workflow is proposed by automatically selecting pseudo-invariant feature (PIF) pixels using DSMs and multispectral satellite images. Then, an improved Dempster-Shafer (DS) fusion model is proposed for building change detection. In this fusion model, five indicators are adopted to classify five kinds of land cover change / non-change situations. The proposed method is applied to industrial areas using IKONOS stereo imagery of two dates. The evaluation result shows the improvement in true-detection-rate compared to the previous approach.**

Keywords—3D; Change detection; buildings; PIFs; Dempster-Shafer.

I. INTRODUCTION

Fast-paced urban and rural development (e.g., urban growth, deforestation) as well as more frequent natural disasters (e.g., earthquakes, hurricanes, tsunamis) have increased the demand for efficient rapid monitoring and disaster assessment. These topics are related to change detection and have led to the establishment of a fundamental research field in remote sensing. Many studies focus on comparing multi-temporal images [1] [2]. However, there are several challenges associated with change detection using only 2D information extracted from satellite images. Limited to the characteristics of optical sensors, only changes related to reflectance values and / or local textural changes can be detected, which often leads to the detection of irrelevant changes between images of two dates.

Therefore, some researches have adopted Digital Surface Model (DSMs) for building change detection [3]-[8]. DSMs from stereo imagery are preferred to LiDAR-DSMs for change monitoring in large area coverage, because of the high acquisition costs of LiDAR data. However, limited to the quality and resolution of DSMs generated from spaceborne data, directly subtracting two Stereo-DSMs does not lead to higher change detection accuracy than using just images. Thus, fusion of the DSMs with the information from original spectral channels of satellite images is necessary to improve the change detection accuracy.

In our previous work [8], an initial Dempster-Shafer (DS) fusion model was proposed. In that fusion model, only three change classes were considered: Building change, surface change, and no-change. Two fusion steps were designed for that approach. In the first fusion step, the height changes and Kullback-Leibler divergence similarity measures between the original images were used as building change indicator. In the second fusion step, vegetation and shadow classifications were used as no-building change indicators for refining the change detection results.

However, more change / non-change possibilities can be presented instead of only three. Therefore, in this paper, an improved DS fusion model is proposed by adopting five indicators to classify five change possibilities. To further improve the change detection accuracy, in the preprocessing step an automatic radiometric co-registration method is proposed. This improved method is tested and compared with our former approaches using a pair of IKONOS stereo imagery. After classification, the building change class is later evaluated by comparing it to the building change reference mask.

II. METHODOLOGY

A. Image Co-registration

The quality of the images from both dates directly influences the performance of any change detection methods. Multi-temporal images which are used for change detection are often acquired under different atmospheric conditions, even by different sensors. Thus, a proper radiometric co-registration is normally necessary to make these images comparable. Two types of radiometric co-registration are employed: absolute radiometric correction and relative correction. Among them, relative correction is normally preferred due to easy and robust performance. A common approach of relative correction is firstly selecting enough pseudo-invariant features (PIFs) [9]. And then a radiometric co-registration can be processed based on these PIF pixels. After this relative correction procedure, the same land cover in the multi-temporal images exhibits similar grey values.

To reach better radiometric co-registration accuracy, these PIFs are normally manually selected according to the following

criteria [10]-[12]: 1) PIFs should not have significant elevation changes from image to image; 2) Regions with potential BRDF (bidirectional reflectance distribution function) effect should be avoided, e.g. vegetation regions; 3) PIFs should be located in flat regions. The manual selection of PIF pixels is time consuming, and difficult to apply for large region monitoring tasks. Therefore, in this paper, an automatic PIFs collection workflow is proposed by using joint information from DSMs and multispectral images.

Firstly the DSMs are used to generate an initial no-change mask. In this step, the robust height difference mentioned in [8] and [13] is adopted. Here a value of 5 meter is chosen as threshold in getting the initial no-change mask. Adopting height information in generating initial no-change masks is faster and results in higher accuracy than using images. This no-change mask is further refined by removing regions with vegetation covers or uneven terrain. Region covered by vegetation can be extracted by calculating the Normalized Differenced Vegetation Index (NDVI) [14] based on the multispectral satellite images. The pixels inside flat terrain regions are defined as pixels with no or low gradient.

For the geometric co-registration, a 3D co-registration method mentioned in [7] is used to remove the spatial shift for all three directions.

B. DS fusion theory

Dempster-Shafer (DS) fusion was introduced by Shafer based on Dempster's rule [15] [16] [17] for the purpose of handling imprecise and incomplete information as well as solving conflicts in information coming from different inputs. Another advantage of DS fusion is that it can handle not only single classes but also the union of several classes [18]. This is particularly useful when change detection is performed for specific objects of interest. For example, NDVI can indicate increasing or decreasing vegetation. Here, vegetation would be a combination of trees, grass and bush classes instead of a single class. Moreover, DS can handle the "mixed" pixel problem, since it can deal with any union of classes [18]. Le Hégarat-Mascle et al. [18] and Rottensteiner et al. [3] have adopted DS fusion for classification of multisource remote sensing images.

DS theory is a belief function-based combination method. Each indicator gives different certainty to each decision class A ($A \in 2^{\Theta}$), 2^{Θ} represent the object classes of interest (such as the building change class) and all possible combinations of them. The certainties of the decision class A are called basic belief mass ($m(A)$), and have values between 0 and 1.

$$\begin{cases} m(\phi) = 0 \\ \sum_{A \in 2^{\Theta}} m(A) = 1 \end{cases} \quad (1)$$

When p indicators are considered, each indicator provides a probability for the classes in B ($B \in 2^{\Theta}$). A and B are two crisp sets and may *e. g.* have an intersection [19][20]. The fused belief mass of A can be represented with DS fusion theory [21] based on:

$$m(A) = \frac{\sum_{B_1 \cap \ldots B_p = A} \prod_{i=1}^{p} m_i(B_i)}{1 - K} \quad (2)$$

i: indicator, and $1 \le i \le p$;

m_i: basic belief mass;

p: number of indicators

$$K = \sum_{B_1 \cap \ldots B_p = \emptyset} \prod_{i=1}^{p} m_i(B_i) \quad (3)$$

K is a measure of conflict among different indicators, meaning that a decision cannot be *e.g.* change and no-change at the same time. $m_i(B_i)$ represents mass functions of indicator i to set B. The basic belief mass shown in Eq. (1) varies in definition for different applications. For instance for height changes: if one pixel has less than 1 m height change, then it is given a low probability to indicate low significance of real building change, since this value is in the range of DSM-noise. In contrast, if it exhibits more than 10 m height change, it will have a high probability indicating real building change.

The sigmoid curve based mass function calculation method [8] is used to get an 'S' shape with less parameters. The main advantage of the sigmoid curve distribution is that it can expand the middle part of the original feature values. After transforming the obtained values, they are less sensitive to the selected threshold value.

$$P_i(x) = \frac{0.99}{1 + e^{-\frac{x-T}{\tau}}} \quad (4)$$

In Eq. (4), x is the original value of each indicator. For our purpose, we add two parameters T and τ to control the symmetry point and the shape of the sigmoid function. The symmetry point corresponding to the value 'T' indicates a certainty of 50%. Obtaining the parameter T for this value can be treated as a threshold selection problem. For pixels having a value (x) near the selected threshold value ($x \approx T$), the obtained probability of P_i is about 0.5. It indicates 50% of certainty to be assigned to the correct class of interest, which means that these values also have a high risk of raising a false alarm. The more a value deviates from the threshold, the higher is the probability that it is assigned to the correct class.

C. DS fuison model

DS fusion rules have to be designed according to a defined purpose, which is building changes in our case. Height changes and 2D change detection results can be used to indicate building changes. Additionally, land cover classification results from multispectral satellite images, like NDVI, can be a useful indicator in separating building change from vegetation

changes. In our previous work, this vegetation indicator is used as a no-building change indicator. As an improvement, in this work, we only use one fusion model, in which the vegetation indicator is also included.

Table I shows the pixel based decision model used in this paper. In this fusion model, five change classes are considered: new built building (NeB), new trees (NeT), Surface change (SC), no-changed vegetation region (NCV), no-change in no-vegetation region (NC). The five indicators that we used are height changes from DSM ($P_{\Delta H}$), 2D change detection result $P_{\Delta IM}$, vegetation index from date 1 P_{v1}, vegetation index from date 2 P_{v2}, and vegetation changes $P_{\Delta v}$. $P_{\Delta v}$ is calculated from NDVI difference from the two dates.

The purpose of this procedure is to distinguish the building changes from other kinds of change classes. For this purpose, we assume that height change (ΔH) indicates any changes that are influenced by height. Here, these changes are NeB and NeT. For separating change (NeB $\cup$ NeT $\cup$ SC) from no-change regions (NCV $\cup$ NC), Interactively Reweighted Multivariate Alteration Detection (IR-MAD) as proposed by Nielsen [22] is used in this paper. We have adopted all multi-spectral channels in IR-MAD calculation. The result is reprojected to a sigmoid-curve distribution, and recorded as $P_{\Delta IM}$ in Table I. In this fusion model, NDVI is used to separate NeB and NeT. However, NDVI cannot directly indicate tree changes. It is only an indicator of the existence of vegetation. For example, a high NDVI before change indicates a combination of NeB, SC, and NCV. To complete this model, no-change regions are separated into two classes: no-change vegetation region (NCV) and no-change no-vegetation region (NC). As shown in Table I, the relationship among these indicators and change classes are well presented.

The combined belief mass functions are also stated in Table I. A classification map can be generated by comparing these values for each pixel based on a winner takes all strategy. That means a pixel belongs to one class that has the highest possibility in this pixel. In this paper, conflict function *K* is not calculated. As for each pixel, the plausibility (1-*K*) would be the same for all classes. In the classification procedure, we can simply compare the numerators of the combined mass. The value of *K* cannot influence the comparison procedure, and the classification results. Therefore, the proposed classification method can take place without knowing *K*. After this comparison, a classification map can be generated.

TABLE I. DS FUSION MODEL FOR BUILDING CHANGE DETECTION

Type	ΔH	$\Delta irmad$	*NDVI (I)*	*NDVI (II)*	$\Delta ndvi$	*Combined Mass*
NeB(new building)	0	0				$\frac{P_{\Delta H} \cdot P_{\Delta IM} \cdot P_{v1} \cdot (1-P_{v2}) \cdot (1-P_{\Delta v})}{1-K}$
NeT(new tree)	0	0				$\frac{P_{\Delta H} \cdot P_{\Delta IM} \cdot (1-P_{v1}) \cdot P_{v2} \cdot P_{\Delta v}}{1-K}$
SC(surface change)	0	0				$\frac{(1-P_{\Delta H}) \cdot P_{\Delta IM} \cdot P_{v1} \cdot P_{v2} \cdot P_{\Delta v}}{1-K}$
NCV (no change-veg.)	0	0				$\frac{(1-P_{\Delta H}) \cdot (1-P_{\Delta IM}) \cdot P_{v1} \cdot P_{v2} \cdot (1-P_{\Delta v})}{1-K}$
NC (no change-non veg.)	0	0				$\frac{(1-P_{\Delta H}) \cdot (1-P_{\Delta IM}) \cdot (1-P_{v1}) \cdot (1-P_{v2}) \cdot (1-P_{\Delta v})}{1-K}$
NeB $\cup$ NeT	$P_{\Delta H}$	0				
NeB $\cup$ NC				$1-P_{v2}$		
NeT $\cup$ NC			$1-P_{v1}$			
NeT $\cup$ SC					$P_{\Delta v}$	
NCT $\cup$ NC	0	$1-P_{\Delta IM}$				
NeB $\cup$ NeT $\cup$ SC	0	$P_{\Delta IM}$				
NeB $\cup$ SC $\cup$ NCV			P_{v1}			
NeB $\cup$ NCV $\cup$ NC					$1-P_{\Delta v}$	
NeT $\cup$ SC $\cup$ NCV				P_{v2}		
SC $\cup$ NCV $\cup$ NC	$1-P_{\Delta H}$	0				

III. EXPERIENCES

A. Exprimental Datasets

The experimental datasets for this research work consist of one pair of stereo imagery captured at different dates and the corresponding DSMs. The stereo images from two dates are acquired on February 12, 2006 and May 02, 2011 respectively, and both are from IKONOS satellite. The area represents an industrial region in Korea with an area size of 0.6 × 0.6 km² containing a factory center with mainly well separated, regularly shaped smaller size buildings.

The stereo imagery in this test area consists of two IKONOS multispectral and panchromatic images. Both data sets are along-track stereo pairs. The multispectral IKONOS imagery has a ground sampling distance (GSD) of 4 m containing four bands (red, green, blue, and near infrared). The panchromatic images have a GSD of 1 m (Fig. 1a and 1b). The DSMs of all stereo pairs are generated using the Semi–Global-Matching (SGM) algorithm implemented at DLR [7], [23], [24] for dense image matching. The generated DSMs are displayed in Fig. 1c and Fig. 1d. Fig. 1e is the manually extracted change reference map, which can be used to evaluate our change detection results. In this test region, only buildings with size larger than 100 m^2 are investigated.

(a)

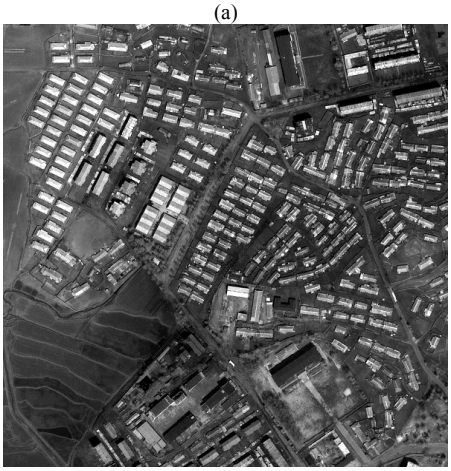

(b)

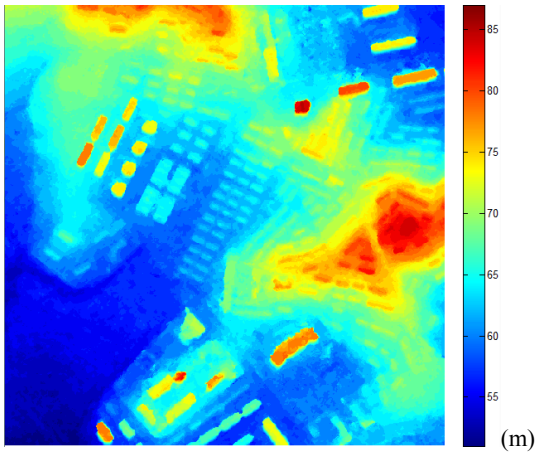

(c)

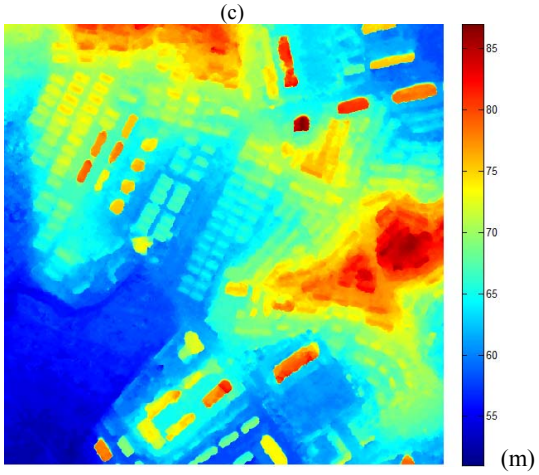

(d)

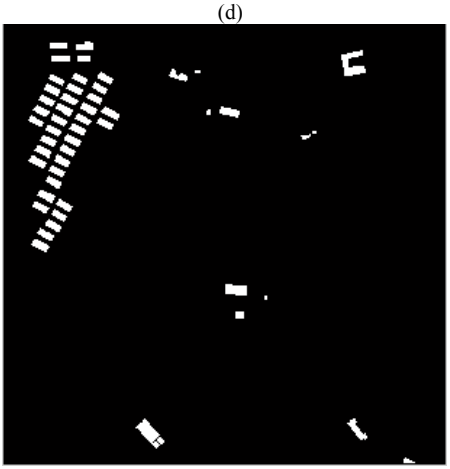

(e)

Fig. 1. Datasets of the test region; (a) panchromatic image from date 1, (b) panchromatic image from date 2; (c) DSM from date 1; (d) DSM from date 2; (e) manually extracted change reference map.

These panchromatic and multi-spectral images are orthorectified using the generated DSMs, meaning that the pixels in the images and DSMs are geometrically co-registered. After orthorectification, all images are resampled to 1 m resolution.

B. Radiometreic Co-registration

The proposed automatic radiometric co-registration method is applied on these data. The automatically selected PIFs are marked in red color in Fig. 2. The corresponding panchromatic image of this region is displayed as background for better understanding. A total of 151,745 pixels remain in the PIF mask.

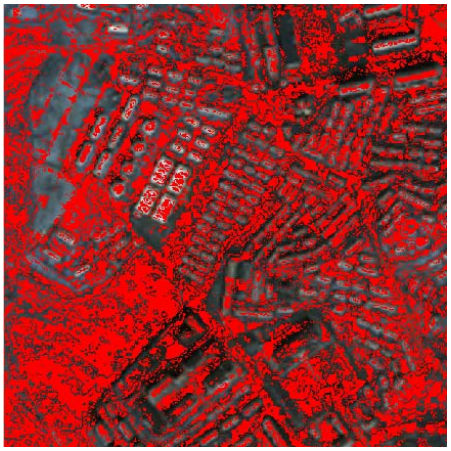

Fig. 2. Automatically selected PIF pixels.

Fig 3 shows the histogram comparison before and after the radiometric co-registration. We take the blue channel as one example. Fig. 3a shows the histogram of PIF pixels before radiometric registration. The red color histogram is the gray value distribution from the blue channel of date 1. The black color histogram represents the gray value distribution from the blue channel of date 2. Even though the original IKONOS images are recorded as 11bits, as can been seen from Fig. 3a, the actual gray value distribution range of the two channels are both lower than 255. Therefore, in the radiometric co-registration procedure, we have scaled both of them to 8 bit images, and then co-registered the PIF pixels channel by channel based on their histograms.

As can be seen, in Fig. 3a the two histograms are totally different. Directly comparing these two images would produce many false alarms. Fig. 3b shows the histograms after radiometric co-registration. In that figure, the two histograms match much better, which means that the unchanged corresponding pixels should exhibit similar gray values.

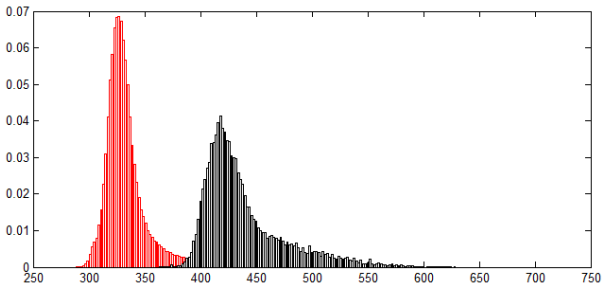

(a)

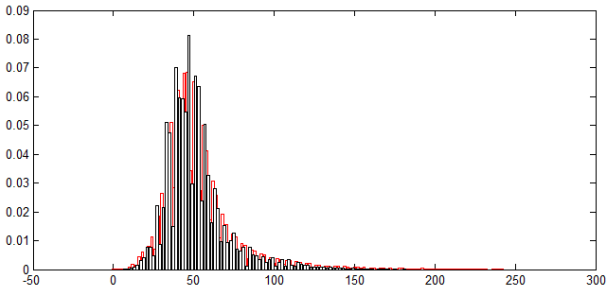

(b)

Fig. 3 Histograms comparison. (a): before co-registration; (b) after co-registration. Red: histogram of blue channel image from date 1; Black, histogram of blue channel image from date 2.

C. Change Detection Results

Based on the proposed DS fusion model, a change classification map of the test area is generated and displayed in Fig. 4. The detected five change classes are shown with five different colors. Among them, the dark blue color indicates the new built building class. To evaluate our detection building changes and the proposed change detection method, the building change class is compared with the change reference map.

Since only changed buildings that are larger than 100 m^2 are considered in the building change reference map, in this paper the detected building mask is further refined by removing regions with an area smaller than 100 m^2. Then, the building change map is overlaid with the building change reference mask. The result is shown in Fig. 5. The green color pixels indicate the true detected, red pixels indicate false alarms, blue color means false negative detections.

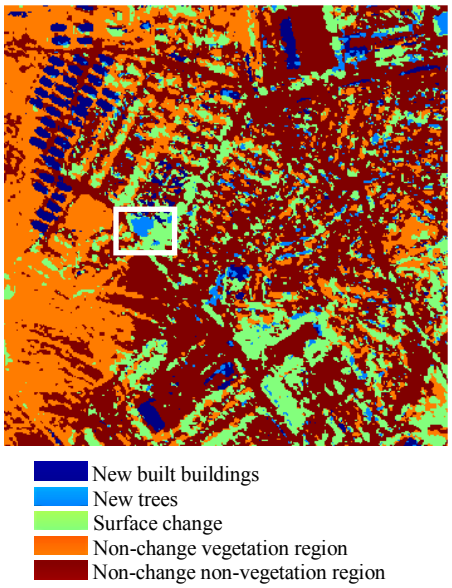

Fig. 4. Change classification map.

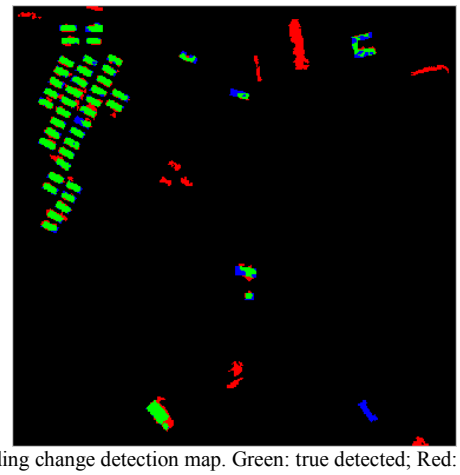

Fig. 5 Building change detection map. Green: true detected; Red: false alarms; Blue: false negative.

TABLE II. CHANGE DETECTION RESULT EVALUATION

Method	True Detected (object)		False Detected (object)	
	Number	Rete[%]	Number	Rate [%]
Ref [8]	42	93.33%	6	15.79%
Proposed	44	97.78%	11	21.57%

Table II shows the object based evaluation result. The proposed method in this paper is compared with the method described in [8]. As it displays, in this test region, 44 out of 45 new built buildings are correctly extracted, which is 2 buildings more than our previous results in Paper [8]. Additionally, a false alarm produced by tree change is successfully removed. As marked with the white rectangular in Fig. 4, the light blue part which was wrongly detected as new built building in [8] is correctly classified as new trees in this result.

Unfortunately, an increased in the false detection rate can be observed. One of the main reasons for these alarms is the DSM quality. For example, the large rectangular shaped false alarm region in the top right side of Fig. 5 is produced due to a matching mistake in generating DSM of date 1. DSMs exhibit relatively bad quality in shadow regions. As no-building change indicators based refinement [8] is not used in this model, false alarms produced by shadows are also remaining in Fig. 5.

IV. CONCLUSION

DS fusion model is a good choice for DSM assisted building change detection. Firstly the DS fusion model is very robust, since after the model is built, it can be easily used for other images in other test regions. Another reason is based on the characteristics of the DSMs from stereo imagery. Height information is essential for urban area monitoring and it is especially helpful for building change detection. Satellite images are easier and cheaper to acquire, but the generated DSMs have potential errors and shortcomings, which means that the height changes obtained from DSM comparison can indicate a building change, but do not directly lead to a reliable decision, which matches with the initial idea of DS fusion.

Generally speaking it could be shown that DSMs generated from space borne stereo data can be a reliable source for efficient building change detection. To fully use all of the change information contained in the original panchromatic images, multi-spectral images and the height information, the DS fusion model has been improved for better separating building changes from other change classes. Additionally, the DSMs and images have been also used together for an automatic radiometric co-registration workflow. The results shows improvements in extracting more changed buildings, but still some false alarms are created by the procedure. A further improvement is therefore required.

REFERENCES

[1] A. Singh, "Digital change detection techniques using remotely-sensed data," International Journal of Remote Sensing, vol. 10 no.6, pp. 989-1003, 1989.

[2] D. Lu, P. Mausel, E. Brondizio, and E. Moran, "Change detection techniques," International Journal of Remote Sensing, vol. 25 no. 12, pp 2365-2407, 2004.

[3] F. Rottensteiner, J. Trinder, S. Clode, and K. Kubik, "Using the Dempster Shafer method for the fusion of LIDAR data and multispectral images for building detection," Information Fusion, vol. 6, no. 4, pp. 283–300, 2005.

[4] N. Champion, F. Rottensteiner, L. Matikaninen, X. Ling, J. Jyyppä and B. P. Olsen, "A test of automatic building change detection approaches," CMRT09. IAPRS, vol. 38, part 3-W4, 2009.

[5] H. Murakami, "Change detection of buildings using an airborne laser scanner," ISPRS Journal of Photogrammetry & Remote Sensing, vol. 54, pp.148-152, 1999.

[6] F. Jung, "Detecting building changes from multitemporal aerial stereopairs", ISPRS Journal of Photogrammetry & Remote Sensing, vol. 58, pp.187-201, 2004.

[7] J. Tian, P. Reinartz, P. d'Angelo and M. Ehlers, "Region-based automatic building and forest change detection on Cartosat-1 stereo imagery", ISPRS Journal of Photogrammetry and Remote Sensing, vol. 79, pp. 229-239, 2013.

[8] J. Tian, S. Cui, and P. Reinartz, "Building change detection based on satellite stereo imagery and digital surface models", IEEE Transactions on Geoscience and Remote Sensing, vol. 52, no. 1, pp. 406-417, 2014.

[9] Y. Du, P.M. Teillet, and J. Cihlar, "Radiometric normalization of multitemporal high-resolution satellite images with quality control for land cover change detection", Remote Sensing of Environment, vol. 82, no. 1, pp. 123-134, 2002.

[10] J.R. Schott, C. Salvaggio, and W.J. Volchok, "Radiometric scene normalization using pseudoinvariant features", Remote Sensing of Environment, vol. 26, no. 1, pp. 1-16, 1988.

[11] D.G. Hadjimitsis, C. Clayton, and A.Retalis, "The use of selected pseudo-invariant targets for the application of atmospheric correction in multi-temporal studies using satellite remotely sensed imagery", International Journal of Applied Earth Observation and Geoinformation, vol. 11, no. 3, pp. 192-200, 2009.

[12] G. Chander, X.J. Xiong, T.J. Choi,, and Angal, A, "Monitoring on-orbit calibration stability of the Terra MODIS and Landsat 7 ETM+ sensors using pseudo-invariant test sites", Remote Sensing of Environment, vol. 114, no. 4, pp. 925-939, 2010.

[13] J. Tian, H. Chaabouni-Chouayakh, P. Reinartz, T. Krauß, and P. d'Angelo, "Automatic 3D change detection based on optical satellite stereo imagery", ISPRS TC VII Vienna ymposium, July 2010, Vienna, Austria,2010

[14] J.W. Rouse Jr, R.H. Haas, J.A. Schell, and D.W. Deering, "Monitoring vegetation systems in the Great Plains with ERTS", Third ERTS Symposium, NASA SP-351, vol. 1, pp.309-317, 1973.

[15] A.P. Dempster, "A generalization of Bayesian Inference", Journal of the Royal Statistical Society, Series B, vol. 30, no. 2, pp. 205-247,1968.

[16] G. Shafer, A Mathematical Theory of Evidence, Princeton University Press, Princeton, New Jersey, 1976.

[17] R. Yager, J. Kacprzyk and M. Fedrizzi, Advances in the Dempster-Shafer theory of evidence, John Wiley& Sons, Inc., New York, 1994.

[18] S. Le Hégarat-Mascle, I. Bloch, and D. Vidal-Madjar, "Application of Dempster-Shafer evidence theory to unsupervised classification in multisource remote sensing," IEEE Trans. Geosci. Remote Sensing, vol. 35, no. 4, pp. 1018–1031, 1997.

[19] D. Dubois and H. Prade, "A set-theoretic view of belief functions Logical operations and approximations by fuzzy sets," International Journal Of General System, vol. 12, no. 3, pp. 193-226, 1986.

[20] D. Dubois and H. Prade, "On the combination of evidence in various mathematical frameworks," Reliability data collection and analysis, Springer, pp. 213-241, 1992.

[21] S. Le Hégarat-Mascle and R. Seltz, "Automatic change detection by evidential fusion of change indices," Remote Sensing of Environment, vol. 91, pp. 390-04, 2004.

[22] A. A. Nielsen, "The regularized iteratively reweighted multivariate alteration detection method for change detection in multi- and hyperspectral data," *IEEE Trans. Image Process.*, vol. 16, no. 2, Feb. 2007, pp. 463–478

[23] H. Hirschmüller, "Stereo processing by semiglobal matching and mutual information," IEEE Trans. Pattern Analysis and Machine Intelligence, vol. 30, no. 2, pp.1-14, 2008.

[24] P. d'Angelo, M. Lehner, and T. Krauss, "Towards automated DEM generation from high resolution stereo satellite images," Proc. ISPRS Congress, Beijing, ISPRS, vol. 37, part B4, pp. 1137-1342, 2008.